

Importance of Clay Minerals in Jordan Case Study: Volkonskoite as a Sink for Hazardous Elements of a High pH Plume

Hani N. Khoury*

Department of Geology, Faculty of Science, The University of Jordan, Amman, Jordan

Abstract

Among the most potential clay deposits in Jordan are kaolinite, bentonite, and palygoskite, volkonskoite, illite, and black mud. A novel geopolymerization process has been recently developed by activating local raw kaolinite to produce green building materials. The clay mineral volkonskoite, a unique green earthy smectite, is widely distributed in central Jordan and is associated with yellow uranium vanadate minerals. Volkonskoite is hosted by altered marble and quaternary thick travertine and recent calcrete deposits. The green clay occurs as thin layers, encrustations and fillings in voids and cavities. The Cr_2O_3 content of the ignited smectites in the new localities ranges between 18.88% and 28.28%. The following are the structural formulae (oxygen = 11) calculated from the microprobe spectral results with the highest and lowest Cr^{3+} content: $\text{Ca}_{0.22}\text{Na}_{0.03}(\text{Cr}_{0.8}\text{Al}_{0.89}\text{Mg}_{0.3})(\text{Si}_{3.92}\text{Al}_{0.08})\text{O}_{10}(\text{OH})_2$ and $\text{Ca}_{0.22}\text{Na}_{0.12}(\text{Cr}_{1.35}\text{Al}_{0.4}\text{Mg}_{0.25})(\text{Si}_{3.68}\text{Al}_{0.32})\text{O}_{10}(\text{OH})_2$. The green clay has uninterrupted continuous flaky texture that confirms their chemical origin.

Most of the travertine caps the varicolored marble zones that were discharged of hyperalkaline ground waters in the past. The varicolored marble (combusted bituminous marl) from central Jordan was altered by the circulating hyperalkaline waters that dissolved Cr^{3+} with other redox sensitive elements, and that was immobilized in Cr-rich smectite – volkonskoite solid solution series. Such waters are similar to the present day active hyperalkaline seepages (pH ~ 12.7) in Maqarin area, north Jordan. The authigenic volkonskoite was formed at a pH similar to the alkali disturbed zone expected at radioactive waste repositories. The Jordanian sites provide the best currently known localities to examine the processes associated with the long-term behavior of radwaste repository sites.

© 2014 Jordan Journal of Earth and Environmental Sciences. All rights reserved

Keywords: clay minerals, central Jordan, chromium rich smectites, hazardous elements, high pH water.

1. Introduction

Jordan is a country rich in clays of different origins. Clays of industrial importance are found in different stratigraphic units from Paleozoic to Cenozoic. The most potential deposits are kaolinite, bentonite, and palygoskite. Other deposits, such as volkonskoite, illite, and black mud, are also widely distributed in Jordan. Details of the occurrence, nature, character, and economic importance of the different clay deposits are given by Khoury (2002 & 2006). Recently, zeolite –A has been synthesized from Jordanian kaolinite (Al-Thawabeia, et al. 2015). Kaolinitic clay, from Jordan, proved to be dioxin-free for in clays feed additives (Alawi *et al.*, 2013; 2014).

A novel geopolymerization process has been recently devised on developing building products (geopolymers) through the geopolymerization of Jordanian kaolinite. The products could be used as low cost construction materials for green housing. They are characterized by high strength, high heat resistance, low production cost, low energy consumption, and low CO_2 emissions. The results confirmed that natural Jordanian kaolinite satisfies the criteria to be used as a precursor for the production of high quality inexpensive, stable materials (Khoury *et al.*, 2011a, 2011b; Rahier *et al.*,

2010, 2011; Slaty *et al.*, 2013; 2015).

Volkonskoite is an important Cr-rich smectite; it was discovered in 1831 by Kammerer in the Okhansak district of perm province of Russia. It was named after Prince A. Volkonskoite, Minister of the Imperial Court (Khoury *et al.*, 1984; Mackenzie, 1988; Eugene *et al.*, 1988).

Volkonskoite is a dioctahedral member of the smectite group that contains chromium as the dominant cation in the octahedral layers. The following is a general chemical formula for volkonskoite (with a molecular weight of 475.69gm.): $\text{Ca}_{0.3}(\text{Cr}^{3+}, \text{Mg}, \text{Fe}^{3+})_2(\text{Si}, \text{Al})_4\text{O}_{10}(\text{OH})_2 \cdot 4\text{H}_2\text{O}$. Volkonskoite has a bright to dark green or emerald green color. In transmitted light, it is emerald green with dull luster. Cr^{3+} is an effective chromophore. In that only small amount, Cr^{3+} gives intensive color to its host mineral (it is used as natural permanent pigment). For this reason, many smectites were called volkonskoite in literature even though their Cr^{3+} content was minor. The term volkonskoite was applied to Cr-bearing smectites with chromium content ranging from 1 % to about 30 % Cr_2O_3 (Foord *et al.*, 1987). Other smectites, with Cr_2O_3 less than 15%, are properly termed chromium montmorillonite, chromium nontronite or are mixture of various chromium-bearing minerals (Foord *et al.*, 1987).

* Corresponding author. e-mail: khouryhn@ju.edu.jo

Volkonskoite is found in Kama river area and Perm basin, as epigenetic minerals commonly filling voids left by the decomposition of plant remains and partly or completely replace organic matter. Cr-bearing smectites have also been formed by the decomposition of ultramafic and mafic rocks in Ural Mountains, Brazil, Bulgaria, Italy, Germany, Norway, Yugoslavia and Nevada. The chromium smectites and chlorites at the Colorado plateau are found in uranium-vanadium deposits and are of epigenetic origin (Foord *et al.*, 1987).

Volkonskoite is widely distributed in central Jordan which could be considered a new type locality for this mineral (Khoury and Abu Jayyab, 1995; Khoury, 2006). Volkonskoite was reported in Daba area for the first time by Khoury *et al.* (1984). More sites have been recently discovered in central Jordan (Khan Ez-Zabib, Tulul Al-Hammam, Siwaqa, and Jabal Al Khurayim area). The structural formulae from these localities are given in Table 1. A new locality has been recently discovered by the author of the present study in Suweileh area, near Amman (Khoury and Zoubi, 2014). The first identified volkonskoite type in central Jordan was characterized to be high chromium, high magnesium and iron free with the following structural formula $[1.06M + (Cr_{2.2}Mg_{2.52})(Si_{7.39}Al_{0.61})O_{20}(OH)_4]$. The chromium content (16%) was higher than that of any volkonskoite yet described from outside the USSR (23.50%) apart from that from Lyalevo, and much higher than that of the samples from the same formation in Palestine (Khoury *et al.*, 1984). Khoury and Abu Jayyab (1995) showed a variation in the Cr content in the octahedral sheets of smectites from different sites from Jordan. The green smectites have different affinities to interlayer cations. They attributed that to compositional variations and/or differences in the layer charge distribution.

Recently, as a result of quarrying and exploration activities of marble, travertine, and surficial uranium deposits in central Jordan, green clays have been found as encrustations and they are associated with yellow uranium minerals (Khoury *et al.*, 2014). The clays together with uranium minerals are hosted by the Pleistocene-Recent travertine and calcrete deposits and the altered part of the underlying varicolored

marble. The Daba (Khan Az-Zabib) and Siwaqa areas, cover 1320 km², and are situated between E36° 00' to 36° 15' and N31° 15' to 31° 45' (Fig. 1). Many tracks leading from the Desert are easily reached from the Amman-Aqaba desert highway, making all parts of the two areas accessible by four wheel-drive vehicles in normal weather. The mean annual precipitation in winter is 110 mm. The mean summer temperature is 23°C with a maximum temperature 44°C and high evaporation rate. The newly discovered clay localities in central Jordan have not been studied before. The following work aims at characterizing the green clayey material from the quarries and trenches mineralogically and chemically, comparing it with that of other localities and at tracing their origin. The importance of the present study lies in introducing the new locality as a natural analogue of engineered barriers in radwaste repository sites.

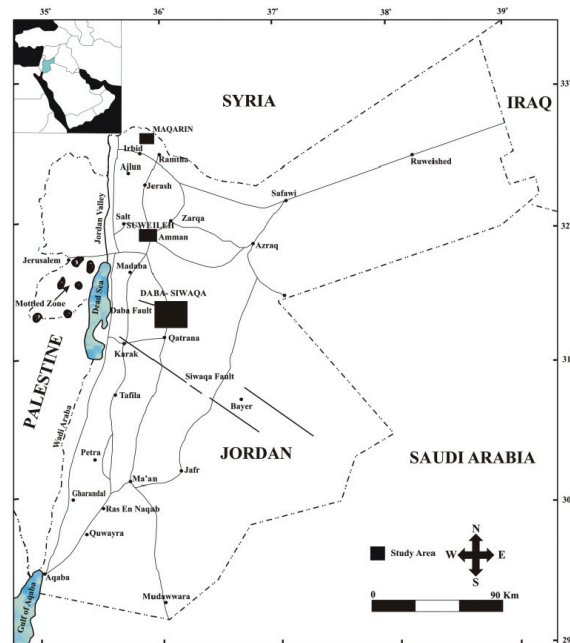


Figure 1: Location map of the study area.

Table 1: Chemical formulae of the studied volkonskoite in Jordan

| Structural Formulae | Location | Reference |
|--|------------------|------------------------------------|
| $-Ca_{0.2}(Cr_{1.1}Mg_{0.4}Al_{0.6})(Si_{3.9}Al_{0.1})O_{10}(OH)_2$ | Uleimat Quarry | Grathoff & Khoury, 2010 |
| $-Ca_{0.3}(Cr_{0.6}Mg_{0.8}Al_{0.7})(Si_{3.9}Al_{0.1})O_{10}(OH)_2$ | -Suweileh | Khoury, 2006; Khoury & Zoubi, 2014 |
| $-Ca_{0.30}Na_{0.23}(Al_{0.47}Cr_{0.63}Fe_{0.13}Mg_{0.66}Zn_{0.06})(Si_{3.88}Al_{0.12})O_{10}(OH)_2$ | -Zmaileh | |
| $-M^{+}_{0.53}(Si_{3.7}Al_{0.3})(Cr_{1.10}Mg_{1.26})O_{10}(OH)_2$ | -Khan Az Zabib | |
| $-Ca_{0.51}Na_{0.03}K_{0.02}(Si_{3.64}Al_{0.036})(Al_{0.08}Ti_{0.02}Fe_{0.08}Cr^{3+}_{0.75}Mg_{1.24})O_{10}(OH)_2$ | -Tlul. Al Hammam | |
| $-Ca_{0.35}Na_{0.02}(Si_{3.71}Al_{0.29})(Al_{0.29}Ti_{0.01}Fe^{3+}_{0.03}Cr_{1.17}Mg_{0.53})O_{10}(OH)_2$ | -Siwaqa Station | |
| $-(Ca_{0.22}Na_{0.03})(Si_{3.69}Al_{0.31})(Al_{0.44}Ti_{0.04}Fe^{3+}_{0.23}Cr_{0.53}Mg_{1.07})O_{10}(OH)_2$ | -Jabal Khreim | |

2. Geology of central Jordan

The geology of central Jordan is illustrated in Fig. 2 and described in details by Khoury *et al.* (2014). The exposed rocks of the studied area (Daba-Siwaqa) are sedimentary and range in age from Upper Cretaceous (Turonian) to Tertiary (Eocene). Pleistocene – Recent travertine, caliche and regolith cover most of the area. The studied area is characterized by unusual colored marble overlain in some areas by travertine and calcrete. The central Jordan varicolored marble is equivalent to the active metamorphic rocks of Maqarin area,

north Jordan. The mineralogy is comparable to that of north Jordan (Maqarin) where present day hyperalkaline seepages circulate through the varicolored marble and bituminous marl. The groundwater discharges today in Maqarin is characterized by high hydroxide alkalinity (pH = 12.7), saturation with calcium sulphate and high concentrations of trace elements (Khoury *et al.*, 1992; Khoury, 2012). The alkaline meteoric waters circulate through the metamorphic zone and precipitate soft travertine and extract redox sensitive elements from the originally combusted bituminous rocks. All the travertine in

the area are recent and are precipitating as a result of kinetic reaction of the hydroxide waters with atmospheric CO₂ (Khoury and Nassir, 1982 a, b; Khoury *et al.*, 1984; Khoury, 1989; Khoury *et al.*, 1992).

The studied area (Daba-Siwaqa) was situated in a shallow marine, stable shelf environment of the Tethys Sea during the Late Cretaceous to Early Eocene (~90 - ~50 Ma ago). Transgression took place during Cenomanian times, and marine sedimentation took place until the Late Eocene, despite the fluctuations in sea level. Uplifting caused gentle folding and faulting that was mostly related to the continued tectonic movement along the Jordan Rift which is located ~60 km to the west of the Daba-Siwaqa area (Bender, 1968; Powell, 1989; Powell and Moh'd, 2011).

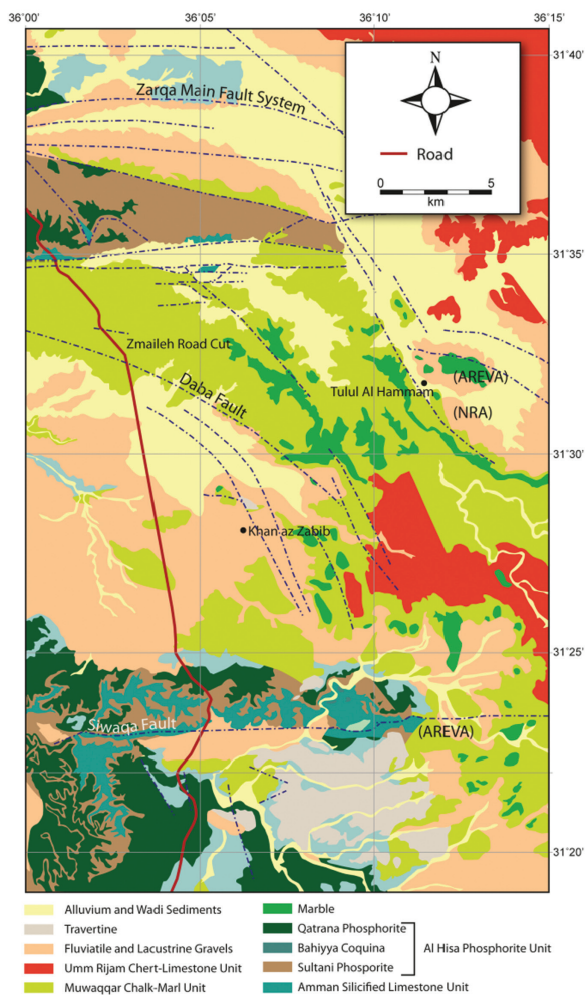


Figure 2: Geologic map of central Jordan (modified after Jasser, 1986; Barjous, 1986; Khoury *et al.*, 2014)

The dominating fault trends are NW-SE and E-W (Fig. 2). The main faults in the area are the Zerqa Main, Daba and Siwaqa fault systems. The fault set is an E-W group of faults and linear features. The folds in central Jordan are of three types: gentle folding associated with regional compression; folding occurring adjacent to faults and directly associated with drag during faulting; and folding in interference structures caused by the interaction of E-W and NW-SE faulting influences (Bender, 1968).

The bituminous marl in central Jordan is biomicrite with average clay content of 10%. Calcite, francolite, quartz, goethite and dolomite are the essential constituents. Framboidal pyrite is found filling the forams cavities. Sensitive

reducing elements as U, V, Zn, Cu, Ni, and Fe are present as sulfides and selenides. U-oxides are mostly adsorbed on the clay minerals and organic matter of the bituminous marl and are soluble under reducing environment. The bituminous marl is overlain by the varicolored marble that is composed of prograde and retrograde metamorphic mineral assemblages ((Khoury and Nassir, 1982 a, b; Techer *et al.*, 2006; Fourcade *et al.*, 2007; Eli *et al.*, 2007). The origin of the extreme polymetallic enrichment (Cd, Cr, Mo, Ni, U, V, Zn) of the Late Cretaceous–Early Tertiary rocks, central Jordan was attributed to the bituminous marl (Fleurance *et al.*, 2012). Combustion of bituminous marl led to decarbonation and formation of prograde metamorphic minerals (recarbonated calcite, spurrite, larnite, etc.) dominated by isotopically depleted carbonates (Khoury, 2006; Khoury *et al.*, 2014). The isotopic evidence supported the high temperature event where the combustion of the organic matter and decarbonation led to the isotopic depletion of $\delta^{13}\text{C}$ and $\delta^{18}\text{O}$. The increase of the temperature of combustion is positively correlated to the enrichment in light stable isotopes (Clark *et al.*, 1993; Khoury, 2006; Khoury *et al.*, 2014). Heating sedimentary apatite up to 800° C indicated a change of color into green, where maximum isotopic depletion took place (Nassir and Khoury, 1982).

Travertines and caliche are mainly composed of calcite. Quartz, opaline phases, and sulphates (gypsum and ettringite) are minor constituents of these rocks. These phases are associated with yellow uranium encrustations and green Cr-rich smectite (volkonskoite) that was reported for the first time in central Jordan by Khoury *et al.* (1984).

The source of Cr, U and V is the bituminous marl. The combustion of the organic matter and the formation of varicolored marble, followed by the action of circulating highly alkaline water, accelerated the leaching of the redox sensitive trace elements. Such an alkaline oxidizing environment (pH~12.7) is currently active in Maqarin area, north Jordan.

The alkaline lakes during Pleistocene Recent time in central Jordan were responsible for the precipitation of travertine as a result of kinetic reaction with atmospheric CO₂. Deflation, local subsidence and the prevalence of dry climate in a later stage led to the concentration of trace elements and the precipitation of calcrete that hosted the Cr-rich clay and uranium deposits (Khoury *et al.*, 2013).

3. Field and laboratory work

Field work has concentrated on sampling the green clays associated with varicolored marble, travertine and calcrete. The green clay is associated with the altered marble. The travertine, several meters in thickness is characterized by the presence of green smectite, coprecipitated with calcite. The excavated trenches indicated the presence of green clay filling the cavities, replacing plant molds, and along bedding planes in travertine and calcrete. Fig. 3 illustrates the green clay with altered varicolored marble (Fig. 3a), filling cavities and replacing plant molds (Fig. 3b), along bedding planes in travertine Fig. 3c) and as encrustation in calcrete (Fig.3d). Most of the travertines are observed capping the metamorphic (cement) zones and contains brecciated blocks of marble.

Fifteen samples of green smectite rich travertine and marl were collected from the recently opened quarries and trenches; seven (Q-samples) from the quarries and seven from the nearby trenches (T-samples). Table 2 gives a list of the

studied samples. The T-samples were collected from a trench excavated by Areva Co. (N 31° 23' 361", E 36° 11' 361"). The Q-samples were collected from a quarry (N 31° 22' 062", E 36° 11' 280"). Fig. 4 illustrates the location of the sampling sites from central Jordan. The samples were characterized using petrological, mineralogical, and chemical methods. The clay size fraction was separated by using Atterberg techniques. Oriented glass slides (dry and glycolated) were prepared. Part of the analytical work (XRD, XRF, SEM) was carried out in the laboratories of the Federal Institute for Geosciences and Natural Resources, Hannover, Germany, and the Department of Geology, Greifswald University, Germany. Infrared spectra were obtained for the whole rock samples using KBr technique (Merlin spectrometer and software). A Philips diffractometer PW 3710 (40 kV, 30 mA) with CuK α radiation, equipped with a fixed divergence slit and a secondary graphite monochromator was used.

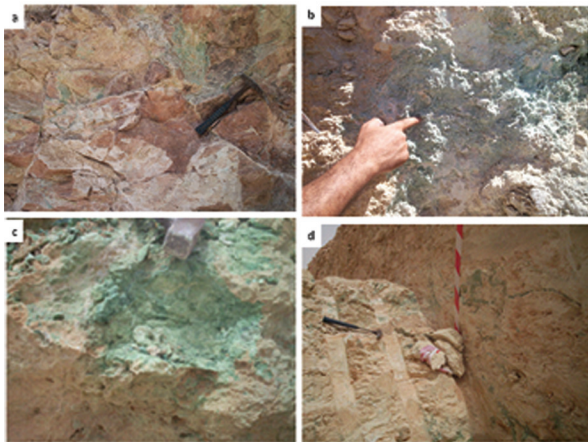


Figure 3: photographs of green clay a) with altered varicolored marble b) filling cavities and replacing plant molds c) along bedding planes in travertine d) as encrustations in calcrete.

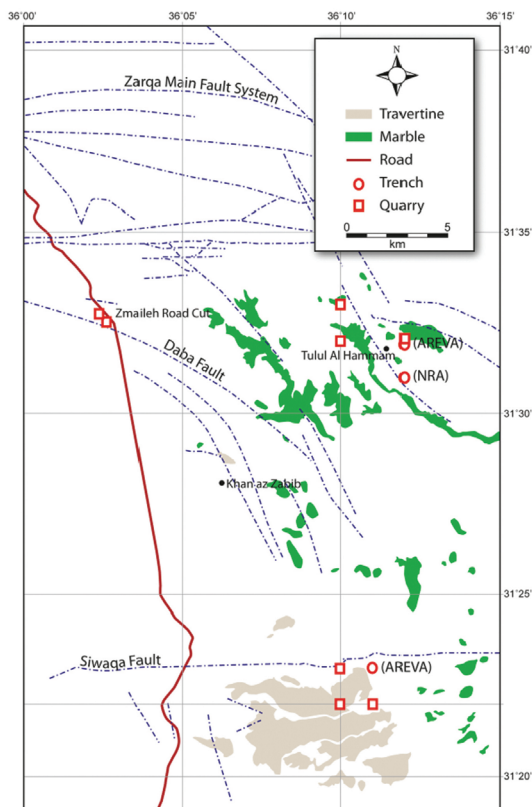


Figure 4: Sampling sites

Table 2: Description of the studied samples.

| Sample No. | Description |
|------------|--|
| Q-1 | Porous travertine with green clay |
| Q-2 | Porous travertine with green clay |
| Q-3 | Porous travertine with green clay |
| Q-4 | Porous travertine with green clay |
| Q-5 | Porous travertine with green clay |
| Q-6 | Porous travertine with green clay |
| Q-7 old | Porous travertine with green clay |
| T2-1 | Yellowish gypsum rich calcrete with green clay |
| T2-3 | Yellowish gypsum rich calcrete with green clay |
| T3-4 | Yellowish gypsum rich calcretewith green clay |
| T3-5 | Yellowish gypsum rich calcrete with green clay |
| T2-6 | Dolomite rich calcrete with green clay |
| T4-1 | Red calcrete with green clay |
| T5-1 | Yellowish calcrete with green clay |
| T5-2 | Green yellow calcrete |

Q = Quarry T = Trench

Whole rock 'random powder' samples were scanned with a step size of 0.02 - 2 theta and counting time of 0.5 s per step over a measuring range of 2–65 2 theta. Powdered samples were analyzed using a PANalytical Axios and a PW2400 spectrometer. Samples were prepared by mixing with a flux material and melting into glass beads. The beads were analyzed by wavelength dispersive X-ray fluorescence spectrometry (WD-XRF). To determine loss on ignition (LOI), 1,000 mg of sample material was heated to 1,030 °C for 10 min. After mixing the residue with 5.0 g lithium metaborate and 25 mg lithium bromide, it was fused at 1,200 °C for 20 min. The calibrations were validated by analysis of reference materials. "Monitor" samples and 130 Certified Reference Materials (CRM) were used for the correction procedures.

Polished thin sections were prepared for all the collected samples for both petrographic, Scanning Electron Microscopy, Energy-Dispersive X-Ray spectroscopy (SEM/EDS), and microprobe analyses. This part of the laboratory work was accomplished at the Department of Earth Sciences, University of Ottawa. All green clay rich samples were chemically spot analyzed using scanning electron microscope attached with Oxford INCA large area SDD detector (quantitative analysis of elements for Be to U). The SEM/EDS analyses were done on fine clay crystals. A JEOL 6610LV SEM was used for studying and analyzing the clay phases. A JEOL 8230 Super Probe for quantitative chemical analyses and images of the green clays was used. The electron microprobe is fitted with five WDS spectrometers and a high count-rate Silicon Drift Detector (SDD) EDS spectrometer.

4. Results

The petrographic results indicated that calcite and carbonate-fluorapatite are the essential constituents of the altered varicolored marble. Travertine is mainly composed of micro to cryptocrystalline calcite. Calcite moulds and replacement of vegetation are typical for travertines (Fig. 5a). Smectite, possibly volkonskoite represents the green secondary clay mineral. Mineralized plant molds, replaced by Cr-smectite and calcite are common (Fig. 5b, c). Opaline silica in travertine is common and indicates a later stage of direct precipitation in weakness zones (Fig. 5d). Ettringite, gypsum, fluorite, opal-CT, and secondary apatite are common. The calcrete is mainly composed of calcite and gypsum. Other carbonates (vaterite and aragonite) in addition to secondary calcite were identified from the XRD patterns. Secondary

green Cr-rich smectite and yellow uranium minerals are common in voids and weakness zones of both travertine and calcrete.

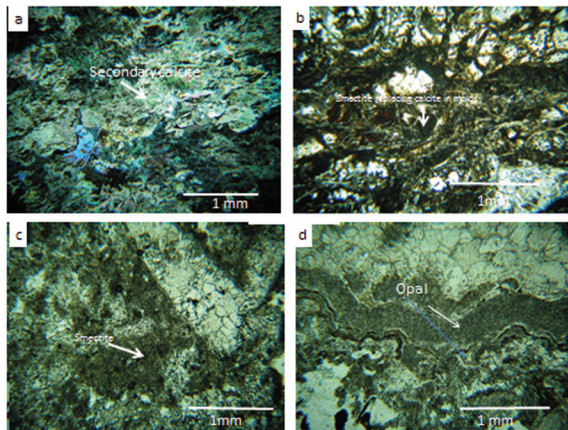


Figure 5: Photomicrographs of a) secondary calcite and replacement of vegetation moulds is typical for travertine (XPL) b, c) mineralized plant molds, replaced by Cr-smectite and calcite are common (PPL) d) opaline silica replacing calcite (PPL)

The secondary green clay from the encrustations, veins of altered marble, travertine, and calcrete was identified from the oriented XRD patterns. The XRD results confirmed the presence of smectite as the essential clay mineral. The XRD basal reflections were constant in all the studied samples. Tyuyamunite, strelkinite, halite and fluorite are associated with the encrustations in the calcrete trench samples. Fig. 6 illustrates a representative XRD pattern of oriented sample of the separated clay fraction. All patterns were identical. The first basal reflection (001) of the dry preparations appears at 12.9 Å and expands to 16.6 Å upon glycolation. The smectite is well ordered and all the basal reflections up to (004) were recorded. The results of the IR spectra of the whole rock samples also confirmed the presence of smectite. Fig. 7 is a representative pattern, illustrating the IR spectra of the minerals in the whole rock samples. This figure illustrates the presence of smectite in addition to calcite and apatite.

The scanning electron micrographs (SEM) photomicrographs indicated that Cr-rich smectites / volkonskoite and the opaline phases are present within the travertine filling voids and cavities and are considered as secondary phases. Opaline phases, however, occur within the some casts of vegetation roots (Fig. 8a). The SEM image indicated that smectite has a cellular and continuous uninterrupted texture (Fig. 8b). The uninterrupted continuous flaky growth of the smectite indicates a chemical origin. The opaline phases associated with the green clay are of late authigenic origin (Fig. 8c). The opaline phases form hexagonal nano-tubes (Fig. 8d).

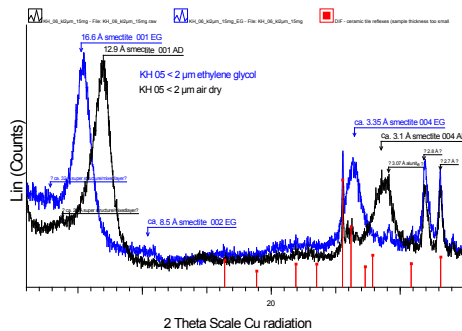


Figure 6: Representative XRD pattern of the studied samples

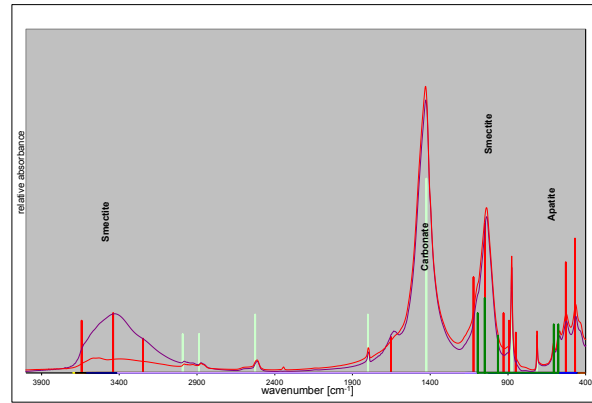


Figure 7: Representative infrared spectra (IR) of the studied samples.

Tables 3 and 4 represent the chemical composition of the major oxides and trace elements of clay hosted travertines and calcrete samples. The CaO and LOI values in Table 3 are related to calcite, apatite and gypsum. The P₂O₅ and F values are related to apatite. SiO₂, Cr₂O₃ and MgO are related to the presence of smectite. The CaO and LOI relationship is plotted in Fig. 9a. The SiO₂ and Al₂O₃ relationship is plotted in Fig. 9b. The MgO and Al₂O₃+Cr₂O₃ relationship is plotted in Fig. 9c. The relatively low positive correlation in these figures is related to the presence of other different phases as calcite, apatite and gypsum. Table 4 shows that the samples are enriched in trace elements as Cr, U, V, Sr, Zn, Zr and Ni up to 7.46 wt. %, 419ppm, 0.74 wt.%, 1042 ppm, 1603 ppm, 117ppm, and 1095ppm, respectively. Cr together with the other elements is considered as redox sensitive elements and is possibly absorbed by smectite. Cr values are related to the presence of Cr-rich smectite as indicated from the EDX/EDS, XRF (clay fraction) and electron microprobe results. The chemical composition agrees with the XRD results of the whole rock samples.

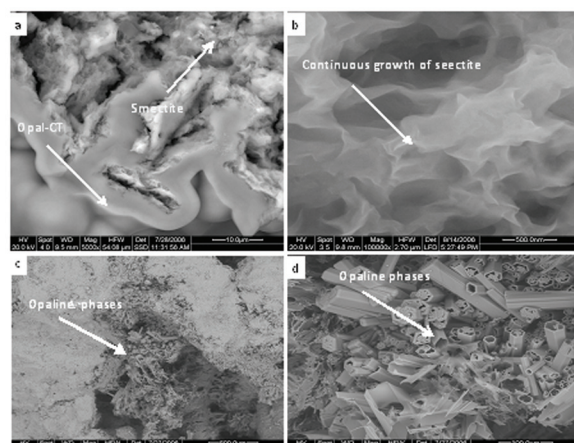


Figure 8: Scanning electron micrographs a) opal-CT with volkonskoite b) continuous growth of volkonskoite c) later authigenic opaline phases d) opaline silica tubes (Khoury, 2012)

Table 3: XRF results of the whole rock samples (Khoury, 2012)

| Sample N | SiO ₂ | TiO ₂ | Al ₂ O ₃ | Fe ₂ O ₃ | Cr ₂ O ₃ | MgO | CaO | Na ₂ O | K ₂ O | P ₂ O ₅ | SO ₃ | F | LOI | Total |
|----------|------------------|------------------|--------------------------------|--------------------------------|--------------------------------|-------|--------|-------------------|------------------|-------------------------------|-----------------|------|-------|--------|
| Q-1 | 10.17 | 0.121 | 2.8 | 1.023 | 3.3 | 0.81 | 42.721 | 0.282 | 0.042 | 0.731 | 0 | 0 | 35.7 | 94.4 |
| Q-2 | 15.37 | 0.143 | 4.19 | 1.397 | 3.49 | 1.378 | 35.894 | 0.513 | 0.103 | 1.192 | 0 | 0.24 | 31.73 | 92.151 |
| Q-3 | 11.71 | 0.11 | 3.33 | 0.987 | 2.3 | 1.093 | 41.512 | 0.429 | 0.044 | 0.986 | 0 | 0.14 | 35.19 | 95.531 |
| Q-4 | 16.58 | 0.16 | 4.38 | 1.123 | 2.26 | 1.55 | 36.187 | 0.242 | 0.035 | 0.875 | 0 | 0.01 | 33.91 | 95.057 |
| Q-5 | 17.63 | 0.082 | 3.22 | 0.611 | 3.59 | 2.603 | 36.464 | 0.195 | 0.03 | 8.063 | 0 | 1.16 | 24.42 | 94.48 |
| Q-6 | 11.78 | 0.085 | 2.69 | 0.609 | 1.84 | 1.895 | 42.82 | 0.156 | 0.034 | 8.63 | 0 | 1.08 | 27.1 | 96.88 |
| Q-7 | 27.39 | 0.179 | 4.03 | 0.592 | 10.89 | 2.232 | 21.026 | 1.028 | 0.23 | 1.231 | 0 | 0.1 | 27.36 | 85.398 |
| T-4 | 4.99 | 0.05 | 0.83 | 0.26 | 0.77 | 0.458 | 50.491 | 0.042 | -0.004 | 0.914 | 0 | 0.3 | 40.19 | 98.527 |
| T5-2 | 4.95 | 0.066 | 1.5 | 0.542 | 0.68 | 0.668 | 31.978 | 0.207 | 0.044 | 0.771 | 13.44 | 0.22 | 23.32 | 77.717 |
| T2-3 | 11.36 | 0.048 | 1.7 | 0.368 | 3.79 | 2.161 | 28.37 | 0.402 | 0.073 | 1.093 | 2.6 | 0 | 23.45 | 71.635 |
| T3-4 | 5.13 | 0.041 | 1.56 | 0.305 | 3.88 | 0.637 | 31.884 | 0.368 | 0.035 | 1.106 | 20.5 | 0.19 | 25.03 | 86.788 |
| T3-5 | 19.93 | 0.129 | 3.3 | 0.893 | 4.22 | 3.882 | 27.564 | 0.665 | 0.155 | 4.84 | 6.02 | 0.55 | 22 | 89.946 |
| T5-1 | 20.03 | 0.163 | 6.09 | 1.381 | 2.9 | 5.761 | 24.985 | 1.087 | 0.088 | 4.196 | 1.24 | 0.81 | 25.47 | 91.333 |
| T2-6 | 18.11 | 0.044 | 2.06 | 0.278 | 9.21 | 2.924 | 26.348 | 0.588 | 0.085 | 0.488 | 4.15 | 0 | 27.66 | 82.741 |
| T2-1 | 36.04 | 0.414 | 7.58 | 2.676 | 0.09 | 2.131 | 19.562 | 0.943 | 0.471 | 1.793 | 0 | 0.3 | 20.97 | 92.891 |

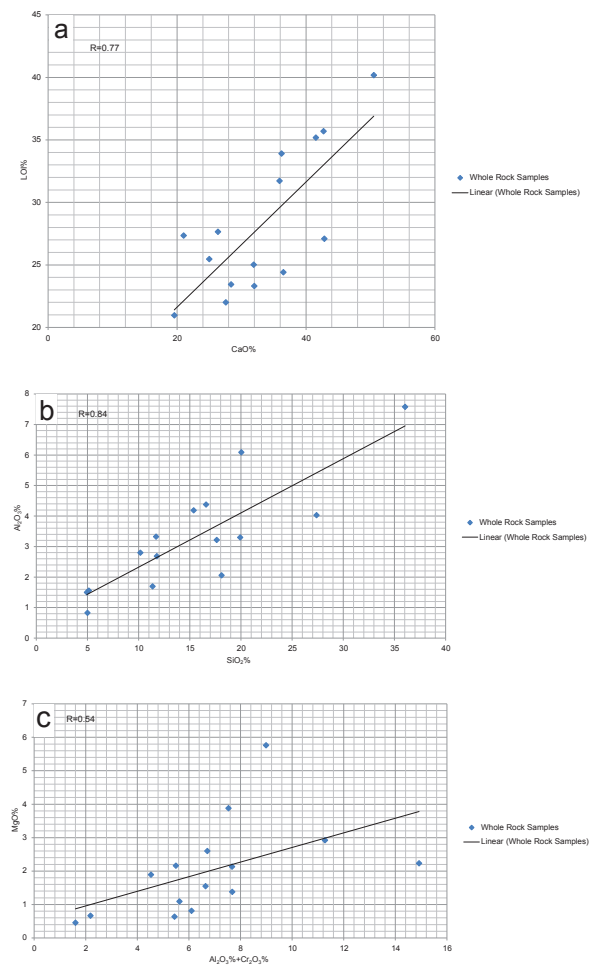
Table 4: XRF results of trace elements in the whole rock samples (ppm)

| Sample | Cr | Ni | Sr | U | V | Zn | Zr |
|---------|---------|--------|--------|-------|--------|--------|-------|
| Q-1 | 17635.6 | 124 | 439.8 | 8.7 | 124.3 | 538.1 | 37.3 |
| Q-2 | 23888.1 | 316.8 | 418.8 | 12.8 | 164.7 | 687.9 | 50.7 |
| Q-3 | 15796.8 | 211.7 | 484.4 | 9.8 | 135.7 | 482.6 | 47.3 |
| Q-4 | 15936.9 | 242.3 | 819 | 8.8 | 142.3 | 245.7 | 78.8 |
| Q-5 | 24640.9 | 277.8 | 600.5 | 37.8 | 193.2 | 417.8 | 65.5 |
| Q-6 | 12660 | 161.6 | 733.9 | 37.1 | 124.5 | 452.5 | 79.7 |
| Q-7 | 74621 | 189.6 | 600.8 | 33.1 | 1117 | 265 | 75.2 |
| T2-1 | 594.3 | 93.2 | 575.3 | 33.5 | 429.3 | 346.5 | 117.6 |
| T2-6 | 63171.4 | 107.3 | 726.8 | 419.4 | 7137.3 | 207.9 | 43.9 |
| T2-3 | 26059.5 | 151.8 | 466.3 | 41.1 | 5235.6 | 3761.3 | 45.6 |
| T3-4 | 26600.4 | 93.5 | 747.9 | 76.9 | 7444.4 | 287.2 | 46.2 |
| T3-5 | 28913.7 | 300.9 | 596.9 | 41.2 | 4217.6 | 1228.7 | 79.5 |
| T-4 | 530.7 | 43.9 | 405.6 | 6.4 | 61.9 | 399.9 | 27.8 |
| T5-1 | 19966.7 | 1095.2 | 1042.9 | 32.9 | 9520.4 | 1603.7 | 114 |
| T5-2 | 4723.1 | 204.6 | 381 | 85.8 | 2023.5 | 222.5 | 46.8 |
| Maximum | 74621 | 1905 | 1042 | 419 | 9520 | 3761 | 117 |
| Minimum | 530 | 44 | 381 | 6.4 | 61.9 | 207.9 | 27.8 |
| average | 23715 | 240 | 602 | 59.02 | 2538 | 743 | 4649 |

Table 5 gives the chemical composition of the major oxides of the separated clay (QU1 samples) and silt (QU2 samples) size fractions of few selected samples. The table indicates the presence of a lot of impurities in the clay fraction as phosphates (Q1-1, Qu1-2, Qu1-3), carbonates (Qu1-4, Qu1-5), and opaline amorphous silica (Qu1-4 and Qu1-5). The silt size fraction is dominated by carbonates as indicated from the CaO content and the high LOI values. Most of the XRD patterns of the clay fraction indicate the presence of smectite, with few crystalline phases as apatite and calcite. It was difficult to calculate the structural formulae of smectites with all these clay size impurities. The poor correlation between the major oxides is related to the presence of impurities. Table 6 gives the XRF results of the trace elements of the separated clay (QU1 samples) and silt (QU2 samples) size fractions of the same samples.

The comparison of the average values of the redox sensitive elements As, Cr, Cu, Ni, U, V, Zn and Zr in both fractions, indicates a higher concentration is in the clay size fraction. The only exception is the higher values of Sr in the silt size fraction, that is related to the presence of calcite.

The SEM/EDS results revealed the presence of almost pure crystallites of smectite (Fig. 10a, b, c, d) and are composed of oxides of SiO₂, Al₂O₃, Cr₂O₃ and MgO. These oxides are the essential components of the smectite. These crystallites were analyzed by the electron microprobe (Fig.

**Figure 9:** Plot of the relationship between a) CaO and LOI b) SiO₂ and Al₂O₃ c) MgO and Al₂O₃+Cr₂O₃.

11). The results are given in Table 7. The following structural formulae were calculated and indicated the substitution of Cr and Mg for Al in the octahedral layer: Ca_{0.22}Na_{0.03}(Cr_{0.80}Al_{0.89}Mg_{0.30})(Si_{3.92}Al_{0.08})O₁₀(OH)₂; Ca_{0.22}Na_{0.12}(Cr_{1.35}Al_{0.40}Mg_{0.25})(Si_{3.68}Al_{0.32})O₁₀(OH)₂. These formulae added more information about the known volkonskoite from other localities in Jordan and support the idea of possible solid solution between dioctahedral smectites (montmorillonite, Cr-smectite and volkonskoite).

Table 5: XRF results in wt% of the major oxides (%) in the (QU1) and silt (QU2) size fractions.

| Sample | SiO2% | TiO2% | Al2O3% | Fe2O3% | MnO2% | MgO% | CaO% | Na2O% | K2O% | P2O5% | SO3% | Cl% | F% | LOI% | Total |
|--------|-------|-------|--------|--------|--------|------|--------|-------|--------|--------|-------|-------|-------|-------|-------|
| QU1-1 | 28.87 | 0.57 | 5.55 | 0.83 | <0.001 | 2.17 | 10.955 | 11.39 | 1.019 | 7.073 | 0.24 | 4.652 | 0.5 | 18.56 | 92.37 |
| QU1-2 | 34.6 | 0.562 | 6.7 | 0.87 | <0.001 | 2.19 | 9.302 | 7.83 | 0.612 | 5.928 | 0.17 | 2.054 | 0.4 | 18.11 | 89.33 |
| QU1-3 | 44.36 | 0.649 | 12.49 | 5.23 | 0.04 | 2.06 | 9.811 | 0.24 | 0.557 | 6.004 | <0.01 | 0.036 | 0.19 | 17.65 | 99.32 |
| QU1-4 | 68.12 | 0.406 | 9.45 | 7.14 | 0.054 | 1.41 | 0.634 | 2.36 | 0.437 | 0.483 | <0.01 | 0.068 | <0.05 | 9.16 | 99.76 |
| QU1-5 | 30.18 | 0.512 | 8.27 | 0.58 | <0.001 | 2.47 | 22.743 | 0.15 | 0.073 | 14.687 | 0.06 | 0.035 | 1.23 | 16.41 | 97.41 |
| QU1-6 | 79.11 | 0.229 | 0.79 | 0.13 | 0.031 | 3.73 | 0.322 | 0.58 | 0.077 | 0.041 | <0.01 | 0.017 | 0.09 | 9.17 | 94.31 |
| QU1-7 | 45.08 | 0.4 | 13.42 | 2.96 | 0.029 | 6.11 | 3.873 | 0.86 | 0.143 | 0.838 | 0.06 | 0.003 | 0.05 | 19.96 | 93.78 |
| QU2-1 | 10.13 | 0.351 | 1.7 | 0.36 | <0.001 | 0.72 | 44.026 | 0.05 | 0.036 | 2.372 | 0.28 | 0.093 | 0.36 | 35.76 | 96.24 |
| QU2-2 | 10.81 | 0.304 | 1.65 | 0.23 | <0.001 | 0.57 | 42.498 | 0.08 | 0.024 | 2.42 | 0.36 | 0.049 | 0.42 | 35.5 | 94.91 |
| QU2-3 | 27.74 | 0.542 | 2.48 | 1.7 | 0.025 | 0.79 | 34.694 | 0.38 | 0.371 | 9.056 | 0.28 | 0.04 | 1.14 | 20.67 | 99.91 |
| QU2-4 | 75.58 | 0.46 | 6.36 | 6.37 | 0.225 | 1.01 | 1.184 | 0.03 | 0.305 | 0.29 | <0.01 | 0.016 | <0.05 | 7.87 | 99.67 |
| QU2-5 | 26.06 | 0.118 | 0.31 | 0.08 | <0.001 | 0.86 | 38.258 | <0.01 | 0.021 | 0.187 | 0.1 | 0.035 | 0.25 | 32.27 | 98.57 |
| QU2-6 | 36.47 | 0.042 | <0.05 | <0.01 | 0.002 | 0.34 | 33.932 | <0.01 | <0.005 | 0.138 | 0.05 | 0.029 | 0.1 | 28.32 | 99.44 |
| QU2-7 | 4.76 | 0.252 | 1.07 | 0.49 | 0.004 | 0.78 | 50.29 | <0.01 | 0.013 | 0.978 | 0.35 | 0.012 | 0.36 | 39.55 | 98.91 |

QU1 = Clay size fraction; QU2 = Silt size fraction

| | | | | | | | | | | | | | | | |
|---------|-------|------|------|------|-------|------|-------|-------|-------|------|------|-------|------|-------|-------|
| AV clay | 47.18 | 0.47 | 6.09 | 2.53 | 0.04 | 2.8 | 6.23 | 3.34 | 0.41 | 5.0 | 0.13 | 0.98 | 0.41 | 15.57 | 95.18 |
| AV silt | 27.36 | 0.29 | 2.26 | 1.53 | 0.064 | 0.72 | 30.62 | 0.135 | 0.013 | 2.20 | 0.23 | 0.039 | 0.43 | 28.56 | 98.23 |

Table 6: XRF results of trace elements (ppm) of the clay (QU1) and silt (QU2) size fractions.

| Sample | As | Cr | Cu | Ni | Sr | U | V | Zn | Zr |
|--------|-----|-------|-----|-----|-----|-----|------|------|-----|
| | ppm | ppm | ppm | ppm | ppm | ppm | ppm | ppm | ppm |
| QU1-1 | 38 | 57062 | 148 | 259 | 347 | 68 | 981 | 171 | 75 |
| QU1-2 | 65 | 73532 | 184 | 363 | 349 | 49 | 1225 | 457 | 75 |
| QU1-3 | 27 | 1929 | 137 | 250 | 302 | 38 | 659 | 1085 | 95 |
| QU1-4 | 24 | 226 | 45 | 65 | 22 | 3 | 299 | 276 | 50 |
| QU1-5 | 4 | 12182 | 181 | 759 | 672 | 79 | 797 | 6357 | 65 |
| QU1-6 | 13 | 35670 | 113 | 226 | 8 | 25 | 115 | 2540 | 4 |
| QU1-7 | 118 | 33542 | 468 | 673 | 80 | 96 | 1475 | 5727 | 65 |
| QU2-1 | 42 | 23314 | 70 | 81 | 482 | 28 | 459 | 207 | 41 |
| QU2-2 | 54 | 31977 | 77 | 86 | 536 | 20 | 528 | 196 | 44 |
| QU2-3 | 8 | 145 | 67 | 52 | 578 | 30 | 147 | 233 | 238 |
| QU2-4 | 19 | 127 | 32 | 68 | 77 | 4 | 275 | 325 | 67 |
| QU2-5 | 9 | 6111 | 38 | 46 | 120 | 42 | 82 | 992 | 17 |
| QU2-6 | 6 | 2894 | 20 | 12 | 119 | 12 | 26 | 197 | <3 |
| QU2-7 | 36 | 2590 | 68 | 105 | 167 | 48 | 336 | 521 | 37 |

QU1 = Clay size fraction; QU2 = Silt size fraction

| | | | | | | | | | |
|---------|-------|-------|-------|-------|-----|-------|-----|------|----|
| AV clay | 41.28 | 30591 | 182 | 370 | 254 | 51 | 793 | 2373 | 61 |
| AV silt | 24.85 | 9594 | 35.14 | 64.28 | 297 | 26.28 | 264 | 381 | 74 |

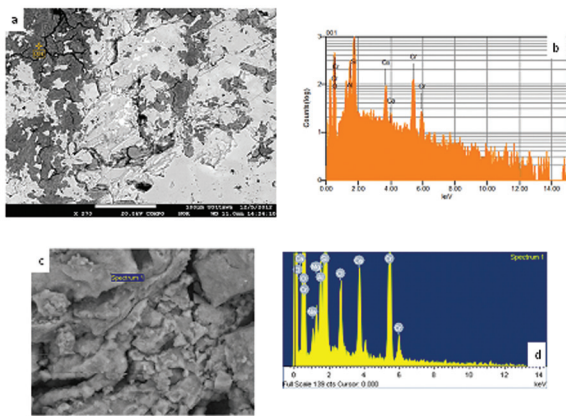


Figure 10: SEM/EDS photomicrographs and spectra of the green clay showing Al, Mg, Cr and Mn as the major components a & b) polished thin section b & d) uncoated sample.

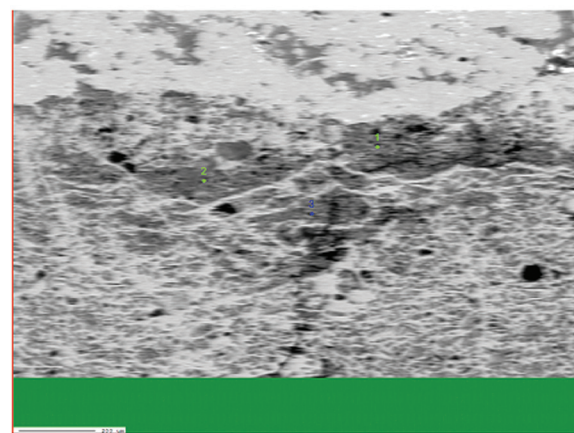


Figure 11: Some selected spots for the electron microprobe analysis.

Table 7: Electron microprobe analyses in wt% of green clay used for the calculation of structural formulae.

| Oxides% | 18 tq-1 1 | 19 tq-1 2 | 20 tq-1 3 | 21 tq-1 4 | 22 tq-1 5 | 24 tq-1 6 | 25 tq-1 7 | 26 tq-1 8 |
|--------------------------------|-----------|-----------|-----------|-----------|-----------|-----------|-----------|-----------|
| SiO ₂ | 45.551 | 51.516 | 39.264 | 51.744 | 45.698 | 49.117 | 40.504 | 53.621 |
| Al ₂ O ₃ | 7.627 | 8.66 | 6.544 | 11.982 | 9.885 | 10.395 | 13.063 | 12.372 |
| TiO ₂ | 0.809 | 0.872 | 0.084 | 0.062 | 0.041 | 0 | 0.027 | 0.091 |
| FeO | 0.102 | 0.095 | 0.04 | 0.178 | 0.134 | 0.05 | 0.079 | 0.133 |
| Cr ₂ O ₃ | 22.295 | 22.953 | 18.21 | 17.34 | 16.393 | 25.439 | 21.067 | 16.764 |
| MgO | 1.975 | 1.923 | 1.746 | 3.411 | 2.959 | 2.22 | 2.299 | 3.934 |
| CaO | 2.471 | 2.492 | 2.259 | 2.197 | 1.932 | 2.559 | 2.633 | 1.816 |
| K ₂ O | 0.039 | 0.06 | 0.038 | 0.075 | 0.071 | 0.026 | 0.013 | 0.039 |
| MnO | 0.017 | 0.028 | 0.022 | 0.018 | 0.02 | 0.027 | 0.007 | 0.015 |
| ZnO | 0 | 0.036 | 0.062 | 0.048 | 0.01 | 0 | 0.071 | 0.033 |
| Cl | 0.959 | 0.481 | 0.555 | 0.486 | 0.52 | 0.144 | 1.092 | 0.161 |
| F | 0.037 | 0.056 | 0.487 | 0.46 | 0.241 | 0.062 | 0.06 | 0.128 |
| SO ₃ | 0.105 | 0.103 | 0.105 | 0.137 | 0.021 | 0.12 | 0.137 | 0.069 |
| P ₂ O ₅ | 0.018 | 0.052 | 0.039 | 0 | 0.046 | 0.02 | 0.104 | 0 |
| Calc Total | 82.26 | 89.58 | 70.13 | 88.25 | 78.16 | 90.44 | 81.68 | 89.46 |

5. Discussion

The XRD basal reflections of the studied Cr-rich smectite/volkonskoite were constant, although the chemical composition and the structural formulae show variation in the Cr content in the octahedral sheets. Specimens from different sites have different affinities to interlayer cations (Table 1; current study). This is attributed to compositional variations and/or differences in the layer charge distribution. The negative charge in the tetrahedral and octahedral sheets is not equally distributed. The differential substitution would result in the variation of the total negative charge within the layers, and accordingly would lead to the variation in the adsorption capacities of the interlayer cations.

Cr-rich smectites/volkonskoite associated with the travertines, calcrete and altered marble in central Jordan were precipitated from ascending high alkaline solution, following the combustion of the original bituminous marls and limestones. The free continuous crystal growth suggests an epigenetic origin and was probably precipitated after calcite and opal. The water chemistry was ideal for the precipitation of the green clay after the removal of CaO and silica from solution (Figs. 5 & 8). The travertine and calcrete were precipitated from highly alkaline groundwater containing calcium hydroxide (pH=12.5) through the uptake of atmospheric CO₂ and subsequent precipitation of calcite (Khoury, 2012; Khoury *et al.*, 2014). Such waters were similar to cement pore water and equivalent to the present day hyperalkaline seepages at Maqarin, north Jordan (Khoury *et al.*, 1992).

The mineralogy of the varicolored marble in central Jordan (Daba-Siwaqa area) is comparable to that of cement clinker and to hydrate cement products (Khoury and Nassir, 1982a, b; Khoury *et al.*, 2014). These rocks are long term natural analogues of Portland cement for sealing of nuclear waste. Premature failure could present serious hazards or release of radionuclides into the environment. Many repository designs, especially those for low- and intermediate-level waste, involve the use of very large amounts of cementitious materials. Bentonite (70% smectite) is one of the most safety-critical components of the engineered barrier system for the disposal concepts developed for many types of radioactive waste (radwaste). The choice of bentonite results from its favourable properties – such as plasticity, swelling capacity, colloid filtration, low hydraulic conductivity, high retardation of key radionuclides and its stability in relevant geological

environments (Alexander and McKinley, 1999). However, bentonite (smectites) are unstable at high pH. The interaction of cement with groundwater results in a hyperalkaline leachate which contains any radionuclides dissolved from the waste. The interaction of such leachate with surrounding rock and the mobility of radionuclides in this complex system must be considered in repository safety assessment. The very slow kinetics of many of the reactions involved, however, greatly limit the applicability of conventional laboratory studies. The varicolored marble, travertines and calcrete of Daba-Siwaqa sites of central Jordan can serve as natural analogues of a cementitious repository. Quaternary travertines capping the metamorphic (cement) zones are the fossilized products of ancient hyperalkaline groundwater discharges (pH ~ 12.7) (Khoury, 2012; Khoury *et al.*, 2014). The travertine and calcrete indicate a long-term analogue of carbonation and remobilization of silica in cementitious barriers for radioactive waste repositories.

Relatively high levels of Cr, Ni, Cu, Zn, U, V, and Zr, are associated with the clay size fraction with the exception of Sr that is associated calcite (Table 6). The presence of Cr-rich smectites - volkonskoite with relatively high levels of U and other redox elements may suggest the use of central Jordan outcrops as analogues with the repository disturbed zone. Smectites are expected to be a sink of alteration products in the late stage evolution of a high pH plume.

6. Summary and Conclusions

The present work demonstrated the value of the altered marble, travertine and calcrete in central Jordan as analogues of cementitious repositories. The sites indicate a long-term analogue of carbonation and remobilization of hazardous elements in cementitious barriers for radioactive waste repositories. The sites offer a good chance to investigate the interaction of the high-pH water enriched with leached hazardous trace elements (Zn, Cr, U, Cu, Ni, V, etc.) with rocks. Heavy metals if removed into groundwater may be hazardous. Co-precipitation of these elements in mineral phases is of great importance to control the concentration of these elements in groundwater. For example, the unusual Cr-smectite - volkonskoite precipitated from the mobile alkaline water may act as sinks for such trace elements.

Mineralogical investigations of natural analogues of cement systems, which underwent reaction with CO₂ over time periods measurable in thousands of years, could give us

an idea about the uptake history of atmospheric CO₂. Central Jordan areas however, represent unique sites to study the durability of Portland cement and concrete, especially for long term assessment of radioactive waste storage. The interface of marble (natural cement zone) overlain by travertine offers large size sampling site which is similar to a sedimentary disposal site. Further investigations of the area and detailed work on the mineral phases in the marble (cement) zone and travertine may aid in understanding the processes likely to occur in the repository near site disturbed zone.

Acknowledgments

The author would like to thank the Deanship of Scientific Research at the University of Jordan for their financial support during my sabbatical year at the Department of Earth Sciences, University of Ottawa, Canada. Thanks are extended to Prof. Ian Clark and Late Prof. Andre Lalonde for supporting part of the analytical work in the different laboratories.

The other part of the analytical work was done at the laboratories of the Federal Institute for Geosciences and Natural Resources, Hanover, and the Department of Geology, Greifswald University, Germany. Special thanks are due to Dr. R. Dohrmann and Dr. J. Grathoff, for their help and cooperation.

References

- [1] Alawi, M., Najjar, A., and Khoury, H., 2013. Analytical Method Development for the Screening and Determination of Dioxins in Clay Matrices. *www. clean-journal.com. Clean – Soil, Air, Water*, 41, 1-7.
- [2] Alawi, M., Najjar, A., and Khoury, H. 2014. Levels of Polychlorinated Dibenzodioxins/Dibenzofurans in Jordanian Clay. *Clean – Soil, Air, Water*, 41, 1-7. DOI: 10.1002/clean.201400240.
- [3] Al-Thawabeia, R., Khoury, H., and Hodali, H. 2015. Synthesis of zeolite 4A via acid-base activation of metakaolinite and its use for water hardness treatment. *Desalination and Water Treatment*. DOI: 10.1080/19443994.2014.941413. (In Publication)
- [4] Alexander, R., and McKinley, M. 1999. The chemical basis of near-field containment in the Swiss high-level radioactive waste disposal concept. pp 47-69 in *Chemical Containment of Wastes in the Geosphere* (eds. R.Metcalf and C.A.Rochelle), Geol.Soc.Spec.Publ. No. 157, Geol Soc, London, UK.
- [5] Barjous, M., 1986. The geology of Siwaqa, Bull. 4, NRA, Amman – Jordan.
- [6] Bender, F., 1968. *Geologie von Jordanien. Beiträge zur Regionalen Geologie der Erde, Band 7 Gebrüder Bornträger*; Berlin.
- [7] Clark, I., Firtz, P. Seidlitz, H., Khoury, H., Trimbom, P., Milodowski, T., and Pearce, J., 1993. Recarbonation of metamorphosed marls, Jordan. *App. Geochem.* 8: 473 - 481.
- [8] Elie, M., Techer, I., Trotignon, L., Khoury, H., Salameh, E., Vandamme, D., Boulvais, P. and Fourcade, S., 2007. Cementation of kerogen-rich marls by alkaline fluids released during weathering of thermally metamorphosed marly sediments. Part II: Organic matter evolution, magnetic susceptibility and metals (Ti, Cr, Fe) at the Khushaym Matruk natural analogue (central Jordan). *Applied Geochemistry*, 22, 1311 - 1328.
- [9] Eugene, E., Foord, Starkey, H., Joseph, T., Taggart, E., and Shawe, D., 1988. Reassessment of the volkonskoite-chromian smectite nomenclature problem; reply, *Clays and Clay Minerals*, 36: 541.
- [10] Fleurance, S., Cuney, M., Malartre, M., and Reyx, J., 2012. Origin of the extreme polymetallic enrichment (Cd, Cr, Mo, Ni, U, V, Zn) of the Late Cretaceous–Early Tertiary Belqa Group, central Jordan, Palaeogeography, Palaeoclimatology, Palaeoecology, <http://dx.doi.org/10.1016/j.palaeo.2012.10.020>.
- [11] Foord, E. E., Starkey, H. C., Taggart, J. E., Jr., and Shawe, D.R., 1987. Reassessment of the volkonskoite-chromian smectite nomenclature problem: *Clays & Clay Minerals*, 35, 139-149.
- [12] Fourcade, S., Trotignon, L., Boulvais, P., Techer, I., Elie, M., Vandamme, D., Salameh, E., and Khoury, H., 2007. Cementation of kerogen-rich marls by alkaline fluids released during weathering of thermally metamorphosed marly sediments. Part I: Isotopic (C,O) study of the Khushaym Matruk natural analogue (central Jordan). *Applied Geochemistry*, 22, 1293 - 1310.
- [13] Grathoff, G., and Khoury, H.N., 2010. A long-term natural analogue for radioactive waste repositories? *Mineralogy and Chemistry of a Volkonskoite (Cr-rich smectite) in Travertine deposits from Central Jordan*.SEA- CSSG- CMS. (Abstract), Trilateral Meeting on clays, Madrid.
- [14] Jasser, D., 1986. The geology of Khan Ez Zabib, Bull. 3, NRA, Amman – Jordan.
- [15] Khoury, H.N., 2002. *Clays and clay minerals in Jordan*, Amman: Special Publication, University of Jordan.
- [16] Khoury, H., 2006. *Industrial rocks and minerals in Jordan* (second edition). Publications of the University of Jordan, Amman.
- [17] Khoury, H. N. 2012. Long-Term Analogue of Carbonation in Travertine from Uleimat Quarries, Central Jordan. *Environmental and Earth Science*. 65:1909-1916. 4.
- [18] Khoury, H., and Nassir S., 1982a. A discussion on the origin of Daba – Siwaqa marble, *Dirasat*, 9 : 55-56.
- [19] Khoury, H. N. and Nassir S., 1982b. High temperature mineralization in Maqarin area, Jordan. *N. Jb. Miner. Abh.* 144, 187-213.
- [20] Khoury, H. N. and Abu-Jayyab 1995. A short note on the mineral volkonskoite. *Dirasat*, No 1, 189-198.
- [21] Khoury, H., and Al-Zoubi, A. 2014 Origin and characteristics of Cr-smectite from Suweileh area, Jordan. *Applied Clay Science*, 90, 43–52.
- [22] Khoury, H. N., Salameh, E. M. and Clark I. D. 2014. Mineralogy and origin of surficial uranium deposits hosted in travertine and calcrete from central Jordan. *Applied Geochemistry*, 43, 49–65
- [23] Khoury, H., Mackenzie, R., Russell, J., and Tait, J., 1984. An iron free volkonskoite. *Clay Minerals*, 19: 43-57.
- [24] Khoury, H. N., Salameh, E., Clark, I., Fritz, P., Bajjali, W., Milodowski, A., Cave, M., and Alexander, R., 1992. A natural analogue of high pH cements pore waters from the Maqarin area of northern Jordan I: Introduction to the site. *Jour. Geoch. Expl.* 46, 117-132.
- [25] Khoury, H., Al Dabsheh, I., Slaty, F., Abu Salha, Y., Rahier, H., Esaifan, M., and Wastiels, J., 2011a. The Effect of Addition of Pozzolanic Tuff on Geopolymers. *The American Ceramic Society Advanced Ceramics and Composites (ICACC), Developments in Strategic Materials and Computational Design II: Ceramic Engineering and Science Proceedings, Volume 32, Issue 10, pages 53-69*. A. Gyekenyesi, W. Kriven, J. Wang, M. Singh (Editors). Wiley. ISBN: 978-1-1180-5995-1.
- [26] Khoury, H., Abu Salha, Y., Al Dabsheh, I., Slaty, Alshaar, M., F., Rahier, H., Esaifan, M., and Wastiels, J., 2011b. Geopolymer Products from Jordan for Sustainability of the Environment. *Advances in Materials Science for Environmental and Nuclear Technology II. The American Ceramic Society: Ceramic Transactions*, 227, 289-300, S. Sundaram, T. Ohji, K. Fox, E. Hoffman (Editors). Wiley, ISBN: 978-1-1180-6000-1
- [27] Rahier, H., Slaty F., Aldabsheh, I., Alshaaer, M., Khoury, H., Esaifan M., and Wastiels J. 2010. Use of local raw materials for construction purposes *Advances in Science and Technology Vol. 69 pp 152-155*. Trans Tech Publications, Switzerland. www.scientific.net/AST.69.152.
- [28] Rahier, H., Esaifan, M., Wastiels, J., Slaty, F., Aldabsheh, I., Khoury H., 2011. Alkali activation of kaolinite for production of bricks and tiles. *Non-traditional cement and concrete IV*, pp.162 - 170, eds. Vlastimil Bilek, Zbynek Kersner.
- [29] Nassir, S., and Khoury, H., 1982. Mineralogy, petrology, and origin of Daba-Siwaqa marble, Jordan. *Dirasat*. 9: 107-130.

- [30] Powell, J.H., 1989. Stratigraphy and sedimentology of the Phanerozoic rocks in central and southern Jordan. Bull. 11, Geology Directorate, natural resources Authority (Ministry of Energy and Mineral resources) Amman, Part B: Kurnub, Ajlun and Belqa group, 161.
- [31] Powell, J. H., Moh'd, B.K., 2011. Evolution of Cretaceous to Eocene alluvial and carbonate platform sequences in central and south Jordan. *GeoArabia*, 16, 4, 29-82.
- [32] Slaty, F., Khoury, H., Wastiels, J H. Rahier ., 2013. Characterization of alkali activated kaolinitic clay. *Applied Clay Science*, 75–76 (2013) 120–125.
- [33] Slaty, F., Khoury, H., Wastiels, J H. Rahier. (2015): Durability of alkali activated cement produced from kaolinitic clay. *Applied Clay Science*. (In Publication)
- [34] Mackenzie, R. C., 1988. Reassessment of the volkonskoite-chromian smectite nomenclature problem; comment. *Clays and Clay Minerals* 36: 540.
- [35] Techer, I., Khoury, H., Salameh, E., Rassineux, F., Claude, C., Clauer, N., Pagel, M., Lancelot, J., Hamelin, B., and Jacquot, E, 2006. Propagation of high-alkaline fluids in an argillaceous formation: Case study of the Khushaym Matruk natural analogue (Central Jordan). *Jour. of Geoch. Exploration*, 90, 53-67.